INTEGRATED CRITERIA AND SYSTEMATIC PROCESS FOR WIND BARRIER INSTALLATION IN STRONG CROSSWIND REGIONS ALONG KOREAN EXPRESSWAYS

Jun Sang Cho
Research Institute of Korea Expressway Corporation, Korea
junsangcho@ex.co.kr
Young Huh
Department of Civil Engineering, University of Suwon, Korea
huhyoung@suwon.ac.kr
Il Keun Lee
Research Institute of Korea Expressway Corporation, Korea
lik@ex.co.kr

ABSTRACT

Korea's expressway network has seen immense expansion in the last decade with connections being made to all provinces and cities. However, on expressways passing through valleys and coastal areas, many stretches are exposed to strong crosswinds. In these regions, sideslips between vehicle tires and the road surface can lead to serious traffic accidents. To reduce accidents, design criteria for the moving speed limit and proper countermeasures such as wind barrier provisions are required.

For this reason, there is a need for integrated criteria and a systematic process that can be incorporated into the Korea Expressway Corporation's policy. In this study, the safety criteria for vehicles under strong crosswinds were established. The design parameters for wind barriers were obtained. This was followed by wind-speed measurements of strong local crosswind fields in all four seasons, which were compared with long-term wind-speed data from the Korea Meteorological Administration. Finally, a systematic process for wind barrier installation was determined based on a probability analysis.

This paper proposes integrated criteria and a systematic process for wind barrier installation in Korea.

1. INTRODUCTION

On expressways passing through valleys and coastal areas, many stretches are exposed to strong crosswinds. In these regions, the sideslips between vehicle tires and the road surface can lead to serious traffic accidents. Although this type of driving vehicle instability has been reported, there have been only a few studies on related criteria or an action plan.

Wyatt [1992] and Smith & Barker [1998] introduced speed limits at the Severn Bridge, Forth Road Bridge, and several other bridges in the U.K. Dellwik et al. [2005]

calculated the time periods with regard to the implementation of restrictions on the Fehmarn Belt Bridge, Oresund Bridge, and Great Belt Bridge in Denmark. Kwon and Jeong [2004] proposed an action plan for speed limits and restrictions on Korean expressways. Wang et al. [2005] presented the wind-speed criteria for the Sutong Bridge in China.

Vehicles running on highways may instantly go out of control owing to strong wind attacks. When cars experience extraordinary wind forces during high-speed driving, there may even be accidents caused by sideslips or overturning of the car body, as shown in Fig. 1. In particular, the risk of car accidents due to strong wind attacks increases on highways in coastal areas, mountain valleys, and along high-rise bridges, as shown in Figs. 2 and 3.

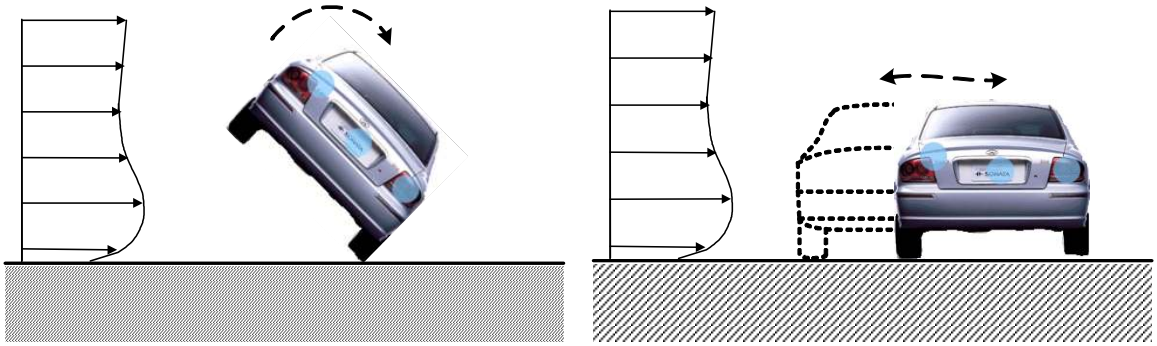

(a) Overturning (b) Sideslip

Fig. 1. Type of driving car failure caused by wind

Overturning and sideslip can be represented as typical accident types when wind blows across the width of the roads. The former can be clearly defined from the equilibrium of forces acting on a vehicle. The latter might cause a collision with other vehicles or a safety barrier.

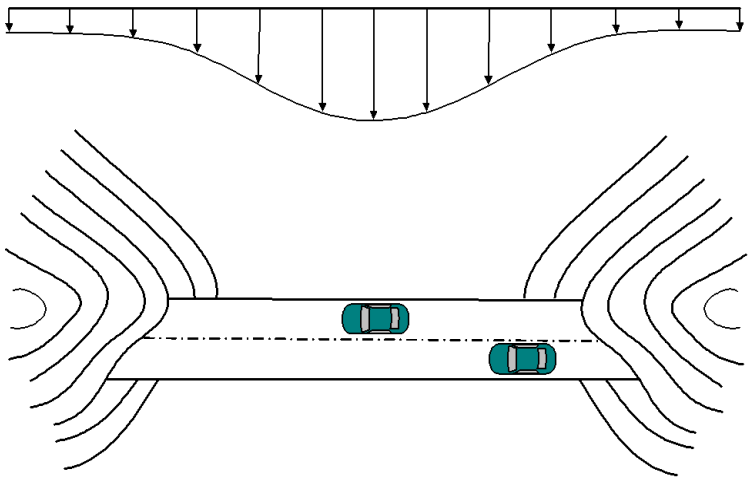

Fig. 2. Wind profile for a deep valley

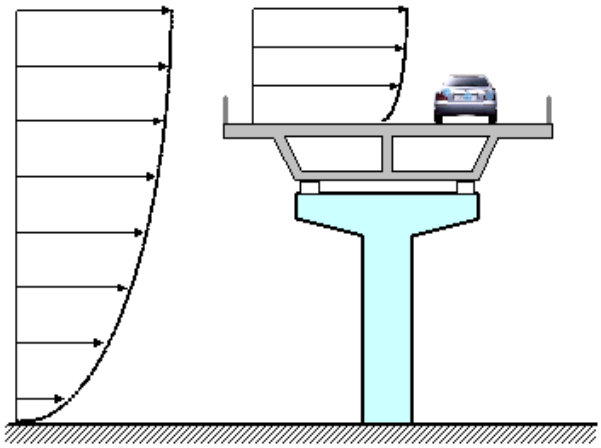

Fig. 3. Wind profile on a high-rise bridge

To develop a reasonable vehicle protection plan to reduce the probability of accident risk, the quantitative relations between the side wind velocity and driving safety must be defined. Then, a strategy to reduce wind force should be proposed. One of the most common methods is to install a wind barrier along roads where strong winds are most likely to occur. However, caution is needed when making a decision on whether a wind barrier is required. Wind barriers should be installed at sites where the car accident risk is high; thus, the risk-based total cost can be reduced in comparison to that when no wind barrier is installed.

In this study, an index to describe car accident risk due to side wind attacks was defined. The dynamic vehicle response was then analyzed by using commercial codes named CarSim and TruckSim [2007], which simulate driving cars under windy conditions. Based on the numerical simulation, the critical wind speed at which cars may fall into a risk state was derived for several types of cars, driving speeds, and road friction. The effect of wind speed reduction by the wind barrier was also investigated by performing a wind tunnel test. In addition, a risk-based life-cycle cost (LCC) analysis was carried out. The total costs for roads both with and without a barrier were calculated and summarized by considering the car accident risk, installation cost, and benefit from the wind barrier. Recommendations were made to install a wind barrier when the total cost could be reduced by the barrier. A wind tunnel test was performed to identify the wind-speed profile behind a wind barrier.

2. RISK ANALYSIS OF DRIVING VEHICLES

2.1. Risk Index

Experimental studies have reported that a driver reacts to sudden extraordinary situations in 0.2~0.4 s [Emmelmann, 1981; Baker, 1986], and moving cars are brought under control in 0.8 s on average. In addition, moving cars may slide twice the distance during that 0.8 s. Thus, the maximum sliding distance due to strong side winds might be doubled during the 0.8 s.

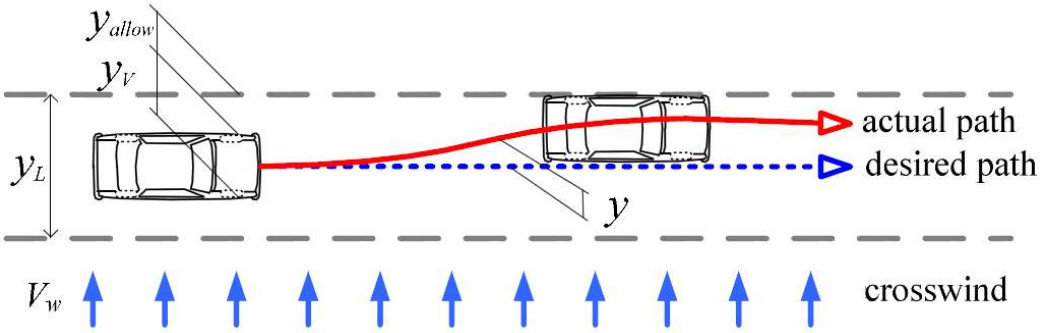

Fig. 4. Vehicle path under crosswind

Fig. 4 shows a plan view of car moving on the road. The safety margin of a car can be defined as

$$y_{allow} = \frac{(Lane\ width - Car\ width)}{2} \tag{1}$$

To decide whether a moving car is at risk or not, the following index is defined.

$$F_y = \sqrt{\frac{1}{1-Y}} - 1 \tag{2}$$

Where $Y = 2y / y_{allow}$. The index F_y is very useful for judging a car's state. For example, if it exceeds 3.0, a car is considered to have run into the adjacent traffic lane.

2.2. Dynamic Analysis

The sliding distance analysis of a moving vehicle during wind attack was carried out by using CarSim and TruckSim. Physical data for cars, trucks, vans, and buses were used as described in the code. In this study, six types of cars(three Hatchbacks, three Sedans), three types of vans(one minivan, two SUVs), and three types of trucks were analyzed. Fig. 5 shows a simulation example for a car.

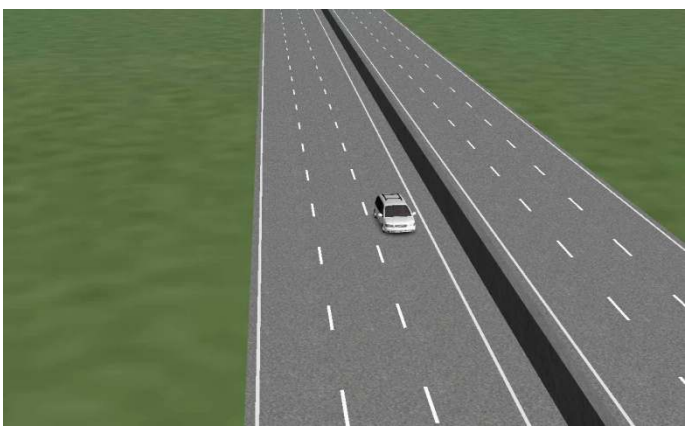

Fig. 5. Simulation of vehicle motion under crosswind by CarSim.

Devices for damping and steering were set as listed in Table 1. When using TruckSim, the steering device was used to prevent excessive sliding distance due to wind.

Table 1. Simulation conditions

Device	CarSim	TruckSim
Damping	Not used	Not used
Steering	Not used	Used

To compare the road state with and without rain, friction coefficients of 0.85 and 0.4 between the tire and road surfaces were considered. The driving speed was increased from 20 to 160 km/h at increments of 20 km/h; in addition, speeds of 90 and 110 km/h were considered. The transverse wind speed was varied from 10 to 40 m/s at increments of 5 m/s. Fig. 7(a) shows the sliding distance according to the driving speed for the car. From the sliding distances, the risk indices for the car were calculated, as shown in Fig. 7(b). When the risk index exceeded 3.0, the car was assumed to be in a risky state. Finally, Fig. 8 and Table 2 show the crosswind speed necessary to cause a sideslip accident, as defined in the previous section [Kwon, 2011].

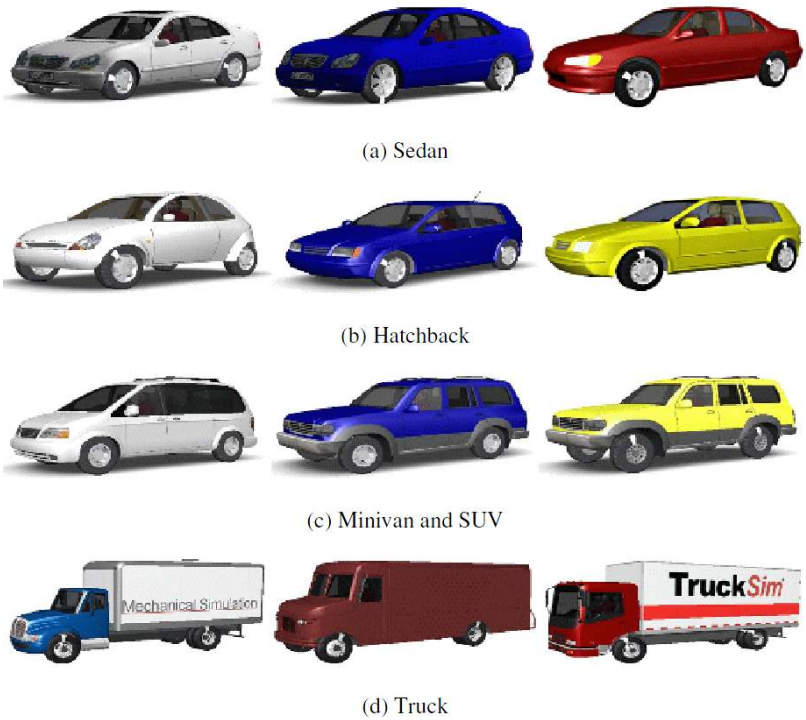

Fig. 6. Vehicle models used in analysis

Table 2. Safety limits speed for driving vehicle models

Vehicle Models	Driving Limits Speed	Wind speed
Sedan, hatchback, minivan and SUV	110 km/h	35 m/s
Bus		30 m/s
Truck	90 km/h	35 m/s

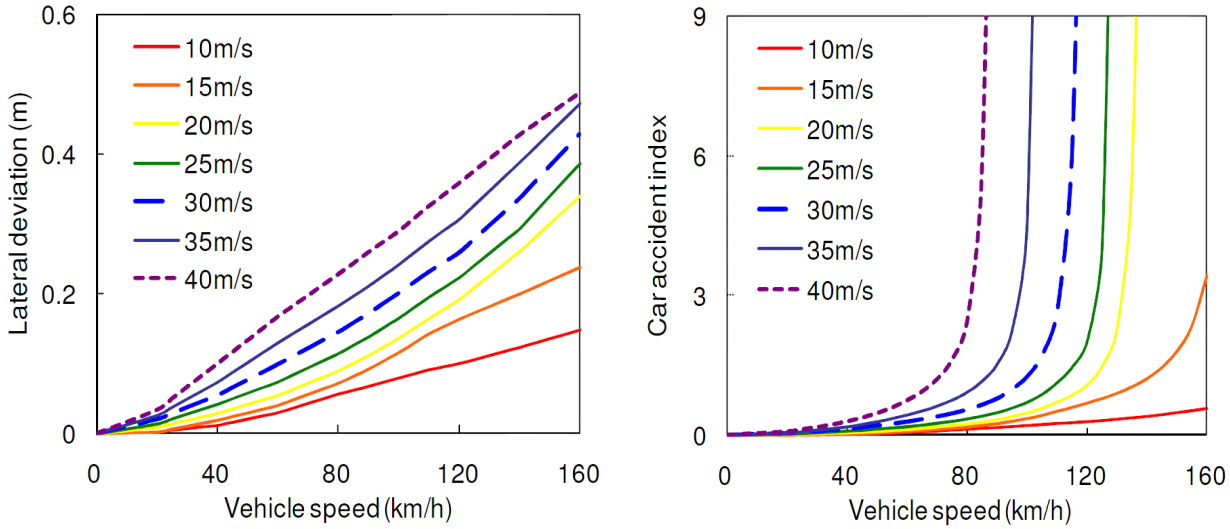

(a) Lateral deviations (b) Car accident indices

Fig. 7. Lateral deviations and corresponding car accident indices for a truck according to wind speeds (dry conditions)

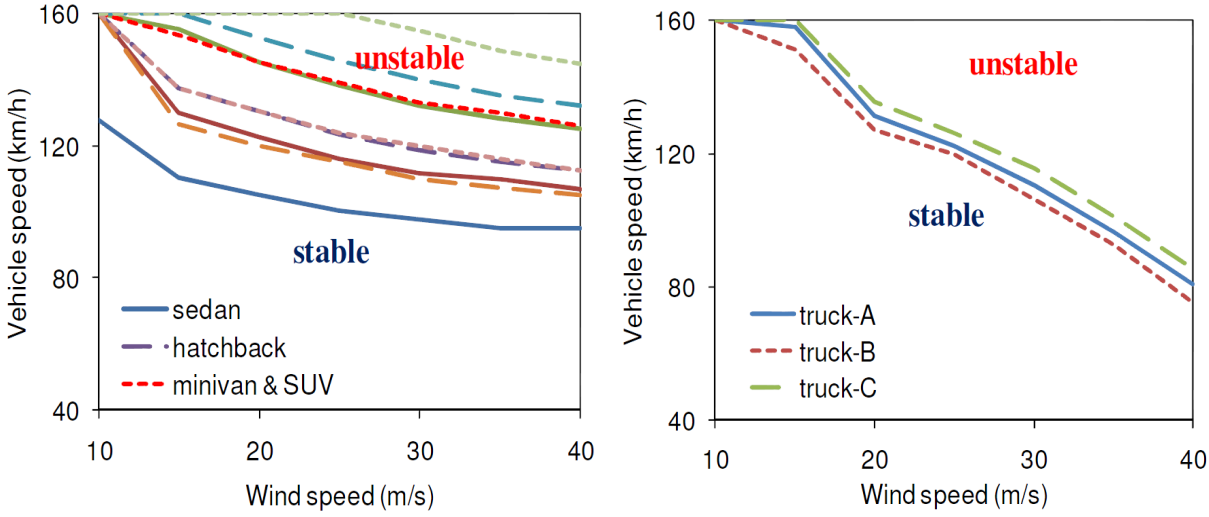

(a) Small passenger cars (b) Truck

Fig. 8. Safety limits for driving stability of road vehicles

3. WIND TUNNEL TEST OF WIND BARRIERS

3.1. Experimental setup

The experiments were performed in a wind tunnel at Chonbuk National University. This closed-return type vertical returning wind tunnel has two test sections. The tests were performed at the low-speed test section of 12 m (W) × 2.5 m (H) × 40 m (L). The wind tunnel has five fans and motors each with a power of 215KW. The free stream velocity of this low-speed test section ranges from 0.3 to 13m/s.

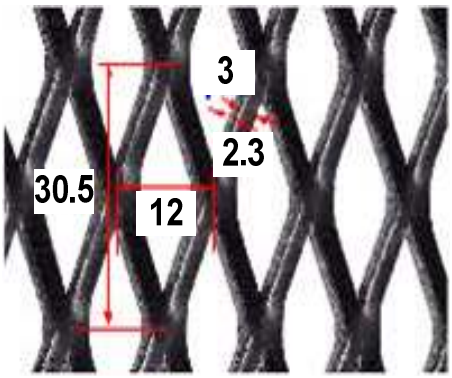

(a) Specifications (units: mm)

(b) Operation on bridges

Fig. 9. Expanded metal barriers

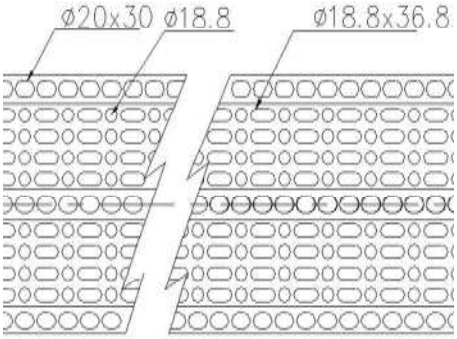

(a) Specifications (units: mm)

(b) Operation on bridges

Fig. 10. Folded porous plate barrier

The natural atmospheric boundary layer flow has differing mean wind speeds and turbulent intensities according to the height from the surface. However, the velocity profile may be considered as a constant value within the barrier height because the height of the target barriers in this study was less than 6 m. Therefore, a smooth flow rather than a boundary layer flow was used in this study to clearly determine the shielding effects of wind barriers.

Two types of wind barriers, which are shown in Figs. 9 and 10, were used. One was made using expanded metal with a porosity ratio of 53.7%, and the other was a folded porous plate with a porosity ratio of 50%. The 14 porosity types of the wind barrier was selected by considering the shielding performance and the driver's visibility from the previous experiments for various porosities [Kwon and Jeong 2004]. The mesh size of the expanded metal and the diameter of the small holes at the folded porous plate were kept the same as those of the actual barriers to prevent possible scaling effects.

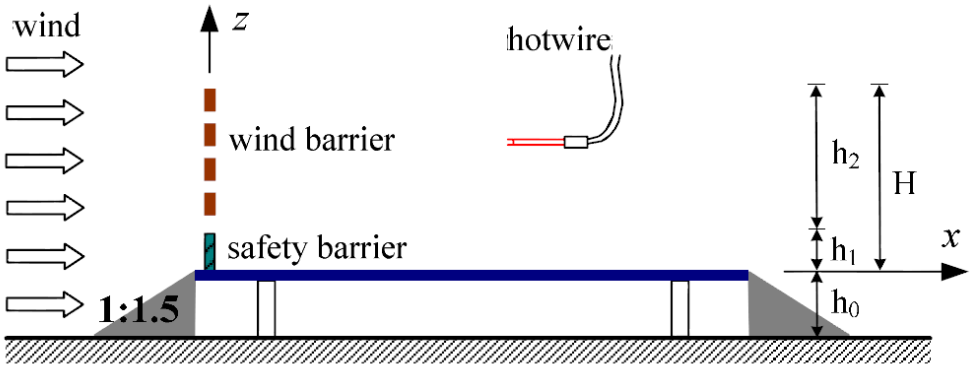

Fig. 11. Schematic diagram of wind barrier arrangements for an elevated bridge and embankment

A schematic diagram of the wind barrier arrangement is shown in Fig. 11. In this study, the model scale was 1/10. The height of the wind barrier was 60 cm, including a safety barrier height of 10 cm. The width of the road was 600 cm, which corresponded to 10 times the barrier height. The tests were performed for two cases: wind barriers installed at an elevated bridge and at an embankment. To simulate the elevated bridge, the bridge deck was lifted up from the wind tunnel floor by 40 cm so that the wind flow could pass beneath the deck. Triangles with a slope ratio of 1:1.5 were added to both sides of the road to simulate the embankment.

The measurements of the turbulent flow were taken along the downstream distance behind the wind barrier for 10 locations and 8 different heights for each location. Thus, the measurements were performed for a total of 80 points. All of the measured data were expressed according to the normalized horizontal distance (x/H) and normalized vertical height (z/H). Here, x is the downstream distance from the wind barrier; H, the height of the wind barrier; and z, the vertical distance from the road. Wind direction was not considered in this study because the wind velocity perpendicular to the road axis is the only important factor that affects the driving stability of vehicles.

3.2. Experimental results

The shelter effect can be determined by the flow reduction which was expressed as the normalized wind velocity (V/V_∞). The normalized wind velocity is the ratio of the mean wind velocity (V) at each downstream station of the wind barrier to the free stream velocity (V_∞). Figs. 9 and 10 show the contour for the normalized wind velocities behind the wind barriers installed at the elevated bridge. As shown in the figures, a significant decrease in the oncoming wind speed after it passes through the barrier can be obtained. In particular, the wind velocities within $x \leq 10H$ and $z \leq 0.8H$ were less than 50% of the free stream velocity.

The normalized wind velocities immediately behind the wind barriers at $x \leq 2H$ did not significantly decrease compared with those at other stations further away from the wind barrier. This is because of the mesh size of the screen. As mentioned in the previous

section, the mesh size of the expanded metal was not scaled down to prevent possible scale effects. The wind velocity immediately behind the wind barrier was not reduced because of the relatively large space between the meshes. The diameter of the holes at the porous plate also played a role similar to that of the mesh size

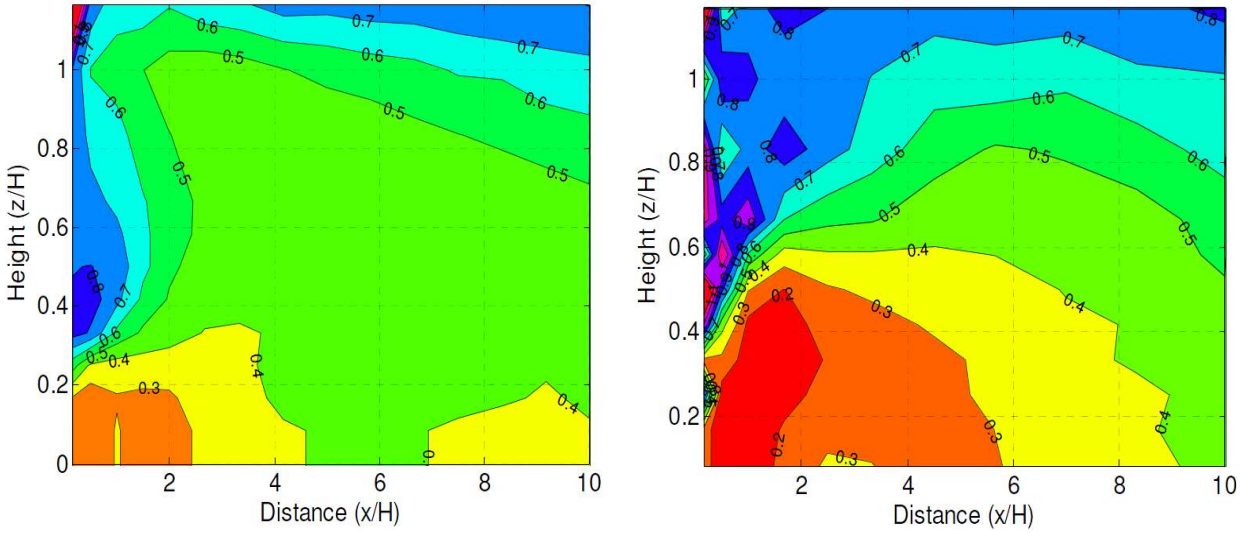

(a) Expanded metal barriers (b) Folded porous plate barrier

Fig. 12. Normalized wind velocities (V/V_∞) behind the wind barrier installed at elevated bridge

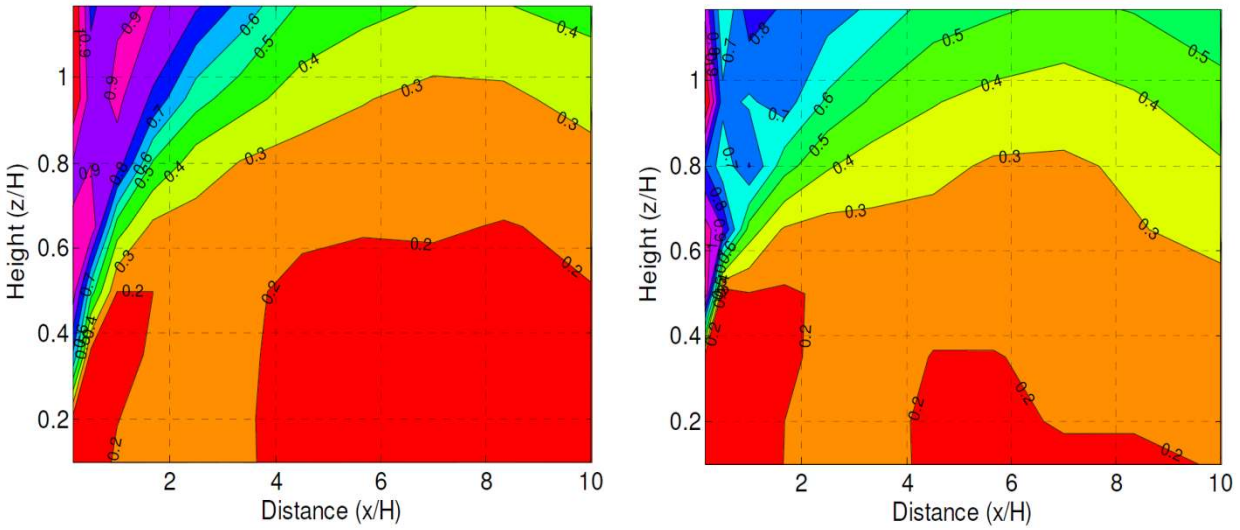

(a) Expanded metal barriers (b) Folded porous plate barrier

Fig. 13. Normalized wind velocities (V/V_∞) behind the wind barrier installed at embankment

The reduction in wind velocities behind the wind barriers caused by both the expanded metal and folded porous plate did not decrease within $x \leq 10H$. The shelter effect was valid for the wind barriers installed at the elevated bridge as well as at the embankment. To summarize the shelter effects, a 50% reduction in wind velocity can be expected within $x \leq 10H$ and $z \leq 0.8H$. Based on the results, the minimum height required for the wind barrier to reduce the wind velocity within the road by 50% can be proposed to be as follows:

$$H_{min} \geq (\text{road width}) / 8 \quad (3)$$

The standard width of an expressway with six traffic lanes in Korea is 30.6 m. Inserting this value into Eq. (3), the minimum height of the wind barrier was computed as 3.83 m, which includes the 1 m height of the standard safety barrier.

4. RISK-BASED DECISION ON WIND BARRIER INSTALLATION

4.1. Probability distribution of wind

The risk-based approach described in detail by Kim et al. [2011] was used to determine whether a site needs a wind barrier. The calculation of the risk-based cost first requires the determination of the probability distribution of wind. Among several extreme value distributions, the generalized extreme value (GEV) distribution of Eq. (4) was used because it best fits the cumulative distribution of wind speed shown in Fig. 14.

$$F = exp\left[-\left\{1 + k\left(\frac{x-\mu}{\sigma}\right)\right\}^{-1/k}\right] \quad (4)$$

Where μ is the location parameter, σ is the scale parameter, and k is the shape parameter.

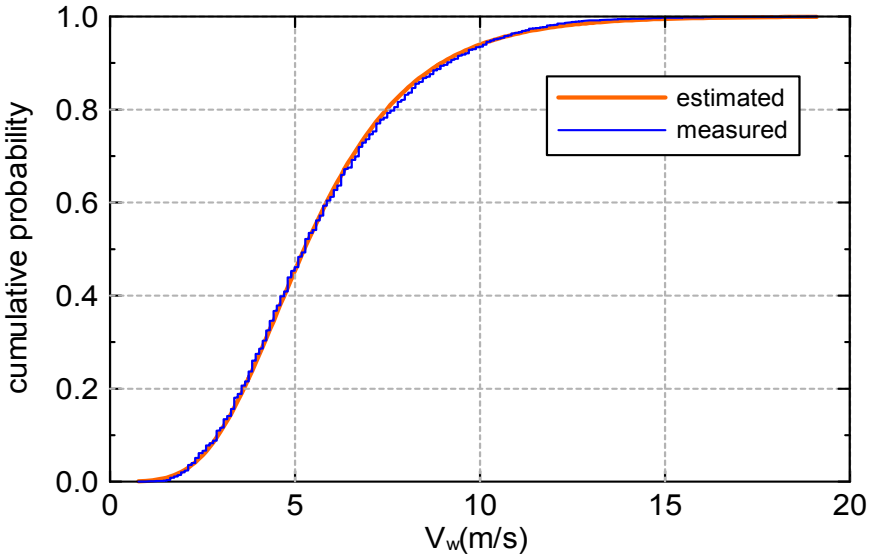

Fig. 14. Cumulative distribution function for GEV

The distribution of wind speed for a road was not available. The measured data plotted in Fig. 14 can only be obtained from weather stations belonging to the Korea Meteorological Administration. Therefore, wind data for a specific site should be estimated by using the data at the stations around the site. The so-called measure-correlate-predict (MCP) method was used in this study to estimate wind data for specific sites. Fig. 15 shows the concept of the MCP method

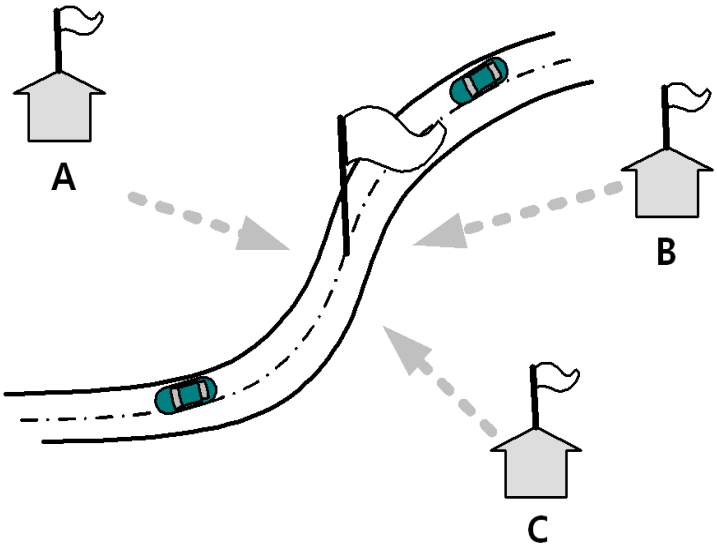

Fig. 15. Concept of wind data estimation

4.2. Calculation of risk-based cost

The probability of failure for a moving car can be defined by the following equation

$$P_f = P_{V_s} P_{AV_s} \tag{5}$$

Where P_{Vs} is the probability of crossing an adjacent traffic lane owing to a strong wind attack, and P_{AVs} is the probability of a car accident when a car crosses the lane. Then, the annual probability of failure can simply be calculated to obtain the expected cost due to car accidents as

$$C_{ai} = N_{ai} \sum_{T=1}^{20} C_{fi} \left(\frac{1+j}{1+r}\right)^T \quad (i = s, v, t) \tag{6}$$

Where N_{ai} denotes the number of annual car accidents; *s, v,* and *t* denote sedans, vans, and trucks, respectively; C_{fi} is the cost of a car accident; and *j* and *r* denote the inflation and discount rates, respectively. In addition, the driving speed limit was increased, though the wind speed would be very high if a wind barrier was constructed at the road. Thus, the time equivalent value can be transformed into a benefit. This can be calculated as

$$B_i = \sum_{T=1}^{20} b_i \left(\frac{1+j}{1+r}\right)^T Q_d r_i \left[\sum_{k=1}^{3} I_{nk} \Delta_{nk} \left(\frac{T_{nk}}{24}\right) - \sum_{k=1}^{3} I_{fk} \Delta_{fk} \left(\frac{T_{fk}}{24}\right)\right] \quad (i = s, v, t) \tag{7}$$

Where b_i is the benefit per car owing to fast driving under strong wind; I_k, the probability of a wind speed between some interval; Δ_k, the driving time for a car; T_k, the lasting time of a certain wind speed range; Q_d, the traffic volume; and r_i, the car mixture ratio. The final cost when a wind barrier is installed can be written as

$$C_i^F = C_l + \sum_l (C_{ai} - B_i) \quad (8)$$

By comparing the cost with and without a wind barrier, we can take a decision whether to install a wind barrier. Of course, the decision should reduce the total cost. Finally, wind barrier installation can be given priority when the ratio B/C is larger than 1.0.

5. INTEGRATED CRITERIA AND PROCESS FOR EXPRESSWAY POLICY

5.1. Criteria for wind barrier installation

5.1.1 *Safety limits wind speed for driving vehicle*

The sideslip caused by crosswinds was computed by using the vehicle dynamics simulation software CarSim and TruckSim, and the critical wind speeds for a car accident were then evaluated from the predefined car accident index. The numerical simulation suggested that the critical gust wind speed for driving stability was 30 m/s for all kinds of vehicles, as listed in Table 2.

5.1.2 *MCP analysis regions along Korean expressways.*

The MCP method uses wind-speed measurements of strong local crosswind fields for all the four seasons, and the obtained data were compared with the long-term wind-speed data of the Korea Meteorological Administration. Strong crosswind areas along Korean expressways were considered for wind barriers if they met the following conditions:

- Strong wind regions according to the Korea Meteorological Administration
- Total length of bridge ≥ 200 m, height of pier ≥ 40 m in valley areas
- Total length of bridge ≥ 200 m in coastal areas

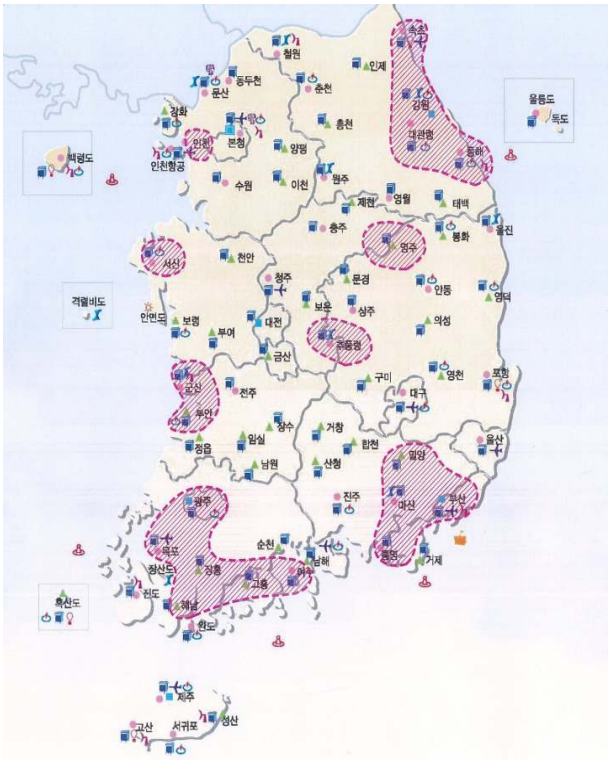

(a) Strong wind regions by KMA

(b) Measurement of wind speed

Fig. 16. Strong wind regions in Korea

5.1.3. *Probability-based decision on wind barrier installation*

GEV functions are widely used to predict wind speed [Gatey and Miller, 2007]. In the Korea Expressway Corporation policy, expressway zones are considered to be dangerous if six or more accidents occur in the zones in a year. For this reason, the probability-based decision-making on wind barrier installation used a recurrence period of 1/6 per year, as shown in Eq. (12).

$$F = exp\left[-\left\{1 + k\left(\frac{v-\mu}{\sigma}\right)\right\}^{-1/k}\right] \tag{9}$$

Applying the GEV function to $V_{1/6}$, we have

$$V_{1/6} = \mu + \frac{\sigma}{k}\left[(-\ln F_{1/6})^{-k} - 1\right] \tag{10}$$

Substituting these expressions into $F_{1/6} = 1 - 6/365 = 0.98356$ and rearranging gives,

$$V_{1/6} = \mu + \frac{\sigma}{k}\left[(-\ln 0.98356)^{-k} - 1\right] \tag{11}$$

Finally, we obtain

$$V_{1/6} = \mu + \frac{\sigma}{k}[(0.01658)^{-k} - 1] \quad (12)$$

5.1.4. *One-side installation by main wind direction*

If the strong wind direction is one-way, it is possible to construct a barrier only on one side of a bridge, as shown in Fig. 17.

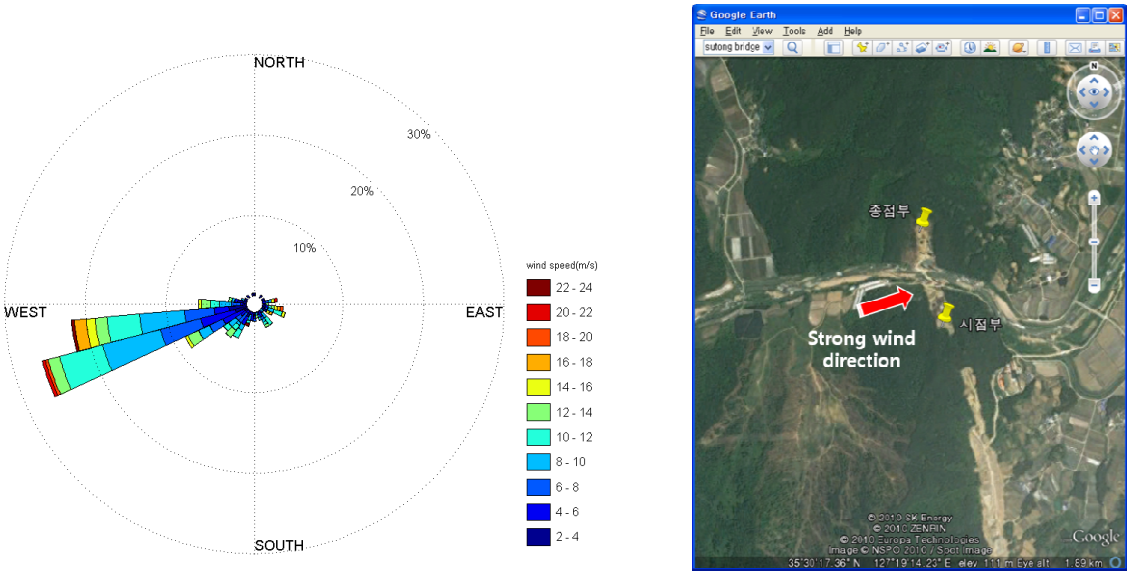

(a) Wind-rose during a year (b) Location when constructing bridge

Fig. 17. Distribution of gust wind direction and speed

5.2. Process for wind barrier installation

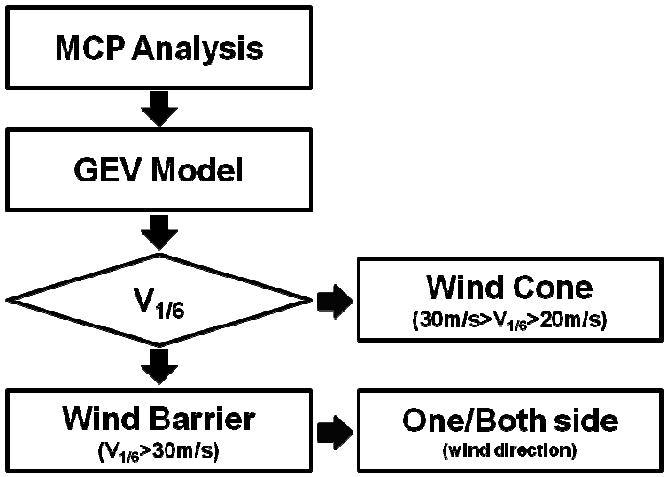

Fig. 18. Process for wind barrier installation

There is a need for integrated criteria and a systematic process that can be incorporated into the Korea Expressway Corporation policy. As described in the previous section, we

developed a process for wind barrier installation, as shown in Fig. 18. In addition, we simulated this process, the details of which are listed in Table 3.

Table 3. Case study for wind barrier installation

Route No.	Name of Bridge	k (shape)	σ (scale)	μ (location)	$V_{1/6}$	Remark
No. 65 (Donghae Expressway)	A	0.0065	2.4684	7.6070	17.86	None
	B	0.0652	4.3977	8.1000	**28.77**	**Wind cone**
	C	0.0652	3.5812	8.4315	**25.26**	**Wind cone**
No. 50 (Yeongdong Expressway)	D	-0.0074	2.7065	8.8957	19.83	None
	E	0.0996	4.3612	9.3448	**31.43**	**Wind Barrier**
	F	0.0996	4.2041	9.2067	**30.49**	**Wind Barrier**
No. 45 (Jungbu Naeryuk Expressway)	G	0.1251	3.2760	7.6783	**25.23**	**Wind cone**
	H	0.0697	2.3980	8.1064	19.49	None
	I	0.0363	2.8236	6.9126	19.39	None
No. 55 (Jungang Expressway)	J	0.0257	2.7632	6.6393	18.59	None
	K	0.0953	2.7758	8.5001	**22.42**	**Wind cone**
	L	-0.0077	2.5080	6.8306	16.95	None

6. CONCLUSIONS

Dynamic analysis of moving vehicles under wind conditions and a wind tunnel test were performed to identify wind speed reduction capability. The results of a numerical study reveals that a transverse wind speed of 30 m/s maintained for an average of 3 s is critical to vehicles running at 110 km/h. The performance of wind barriers in reducing wind speed behind the barrier was verified by performing an experimental wind tunnel test. In addition, a methodology for determining whether to install a wind barrier at a certain site was proposed by using a probability-based decision process.

First, the safety criteria for vehicles under strong crosswinds are established. Following this, the design parameters for wind barriers are obtained. This is followed by wind-speed measurements of strong local crosswind fields in all four seasons and a comparison of the obtained data with the long-term wind-speed data of the Korea Meteorological Administration. Finally, the systematic process for wind barrier installation is determined based on a probability analysis.

This study presents integrated criteria and a systematic process for wind barrier installation in Korea.

ACKNOWLEDGEMENTS

This research was fully supported by the Korea Expressway Corporation in the Republic of Korea.

REFERENCES

1. Wyatt, T.A. (1992), “Recent British developments: Wind shielding of bridges for traffic”, Proceedings of the First International Symposium, Copenhagen, Denmark, February.
2. Smith, B.W. and Barker, C.P. (1998), “Design of wind screens to bridges, experience and application on major bridges”, Proceedings of the International Symposium on Advances in Bridge Aerodynamics, Copenhagen, Denmark, May.
3. Dellwik, E., Mann, J. and Rosenhagen, G. (2005), Traffic restrictions due to wind on the Fehmarn Belt bridge, Risø National Laboratory, Risø-R-1521.
4. Kwon, S.D. and Jeong, U.Y. (2004), “Vehicle protection program against high winds in Korea”, Proceedings of the Bluff Body Aerodynamics & Applcations (BBAA5), Ottawa, Canada, July.
5. Wang, D.L., Chen, A.R. and Pang, J.B. (2005), “Wind speed criteria of driving safety of vehicles on cable stayed bridges”, Proceedings of the Sixth Asia-Pacific Conference on Wind Engineering, Seoul, Korea, September.
6. Mechanical Simulation Corporation (2007), CarSim User manual.
7. Emmelman, H.J. (1981), Driving stability in side winds, Aerodynamics of Road Vehicles, (Ed. W.H. Hucho), Vargel Verlag.
8. Baker, C.J. (1986), “A simplified analysis of various types of wind induced road vehicle accidents”, J. Wind Eng. Ind. Aerod., 22(1), 69-85.
9. Kwon, S. D., Kim, D. H., Lee, S. H. and Song, H. S. (2011) Design criteria of wind barriers for traffic. Part 1: wind barrier performance. Wind and Structures, Vol. 14, No.1 55-70.
10. Kim, D. H., Kwon, S. D., Lee, I. K. and Jo, B. W. (2011) Design criteria of wind barriers for traffic. Part 2: decision making process, Wind and Structures, Vol. 14, No.1 71-80.
11. AASHTO (1989), Guide Specifications for Structural Design of Sound Barriers
12. Abe, M., Kano, Y., Shibahata, Y. and Furukawa, Y. (1999), Improvement of vehicle handling safety with vehicle side-slip control by direct yaw moment, Vehicle System Dynamics, 665-679.
13. Benjamin, J.R. and Cornell, C.A. (1979), Probability, Statistics, and Decision for Civil Engineers, McGraw Hill.
14. KEC (2008), A Study on the Wind Resistance Design Method of the Highway Facilities, Korea Expressway Corporation. ST-08-07
15. MOCT (2007), Design Guidelines of Traffic Facilities Investment, Ministry of Construction and Transportation.